

Subsurface Investigation of Solid Minerals Potential Zones in Northwestern Part of Sokoto Basin Using Aeromagnetic Data

Janet Ronke Olojede¹, Danladi Senchi Bonde², Benjamin Joshua³, Usman A⁴

¹Department of physics, Kebbi State University of Science and Technology, Aleiro, Nigeria

²Department of physics, Kebbi State University of Science and Technology, Aleiro, Nigeria.

³Department of physics, Kebbi State University of Science and Technology, Aleiro, Nigeria

⁴Department of physics, Kebbi State University of Science and Technology, Aleiro, Nigeria

Submission: 18-01-2022

Revised: 28-01-2022

Acceptance: 31-01-2022

Abstract: This present study presents the results of the analysis and interpretation of aeromagnetic data of part of Sokoto basin with the aim of investigating the subsurface structures for solid mineral exploration on a reconnaissance basis. This study employed both qualitative and quantitative interpretation to achieve the aim and objectives of the study. The qualitative interpretation includes; the interpretation of the total magnetic intensity map of the study area, the residual map, first and second vertical derivative maps, tilt derivative map, lineament map. While the quantitative interpretation include the interpretation of source parameter imaging map and Euler deconvolution map for depth estimates. The study area is bounded with Longitude $4.50^{\circ}E - 5.50^{\circ}E$ and lat $12.50^{\circ}N - 13.50^{\circ}N$ with an estimated total area of 12, 100 sq.km. The TMI map is characterised with high and low magnetic signatures with the magnetic signatures ranging from a low magnetic field value of -42.46 nT along western region to some part of northern and south eastern region of the study area, to a high magnetic field value of 133.30 nT in the southwestern, north-eastern and north western parts of the region. While the magnetic values of the residual field obtained from regional/residual separation ranges from -77.31 nT to 61.34 nT. The results of the digital filter used in this study show that major structures such as faults, fractures and shear zones which might host potential solid minerals within the study area trend NW-SE, NE-SW. The results of the depth estimating techniques employed reveal thickness of sediments depicted with an average thickness of 1.8 km and shallow depth of 0.14 km at the northern, southwestern and south-eastern part of the study area. Since structures within the crystalline rocks are the host of some magnetic

minerals, the average depth at which this could be located is about 0.14 km. It can therefore be concluded from this study that the results of the analysis and interpretation of aeromagnetic data of part of Sokoto basin with the aim of investigating the subsurface structures for solid mineral revealed the regions of possible mineralisation and the depth at which they can be explored has been successfully delineated.

Keywords: Total magnetic intensity, Residual magnetic intensity, analytic signal, tilt derivatives, Euler deconvolution, source parameter imaging.

I. INTRODUCTION

Minerals are naturally occurring substances that have characteristic chemical composition and in general, a crystalline structure. Solid minerals are natural resources that form part of the earth resources which beckon human race for exploitation, extraction and utilization. Nigerian is endowed with several mineral resources spread across the length and breadth of the country. These mineral deposits include platinum, iron, tantalite and columbite, tin, granite, marble gypsum diamonds, gold, kaolin, coal, limestone, alluminiumate (Sada, 2013). Nigeria is a country blessed with various mineral resources buried beneath the surface of the earth, but Nigeria depends solely on the crude oil. Thus, solid minerals exploitation has been advocated as a means to diversifying the Nigerian economy away from crude oil, Aigbedion and Iyayi (2007)

Ajaka and Oyathelemi (2010), detailed on the location of solid minerals in Nigeria it was mention in the study that the exploitation of solid minerals would contribute immensely to the national wealth with associate socio-economic benefits.

The aeromagnetic survey is the oldest potential field method used for hydrocarbon and minerals exploration. The main purpose of the aeromagnetic survey is to detect minerals or rocks that have unusual magnetic properties which reveal them by causing anomalies in the intensity of the earth magnetic field (Reeves, 2005). The aeromagnetic survey is applied in mapping these anomalies in the earth's magnetic field and this is correlated with the underground geological structure faults which usually show up by abrupt changes or close spacing in orientation of the contours as revealed by the magnetic anomalies. For minerals and intrusive rocks, residual magnetic anomaly maps are useful since such maps help to identify the presence of intrusive lava flows, or

igneous plugs. The sedimentary formation has shown great potentials for natural resources observed from extensive geophysical investigations (Eze, 2011).

The present study intends to use some software techniques of data management and interpretation to evaluate the magnetic anomalies of the Northwestern parts of the Sokoto basin, Nigeria, which can help predict the solid minerals potentials of the area.

II. LOCATION OF THE STUDY AREA

The study area consists of aeromagnetic sheets covering Binji sheet (9), Sokoto sheet (10), Argungu sheet (28) and Dange sheet (29).

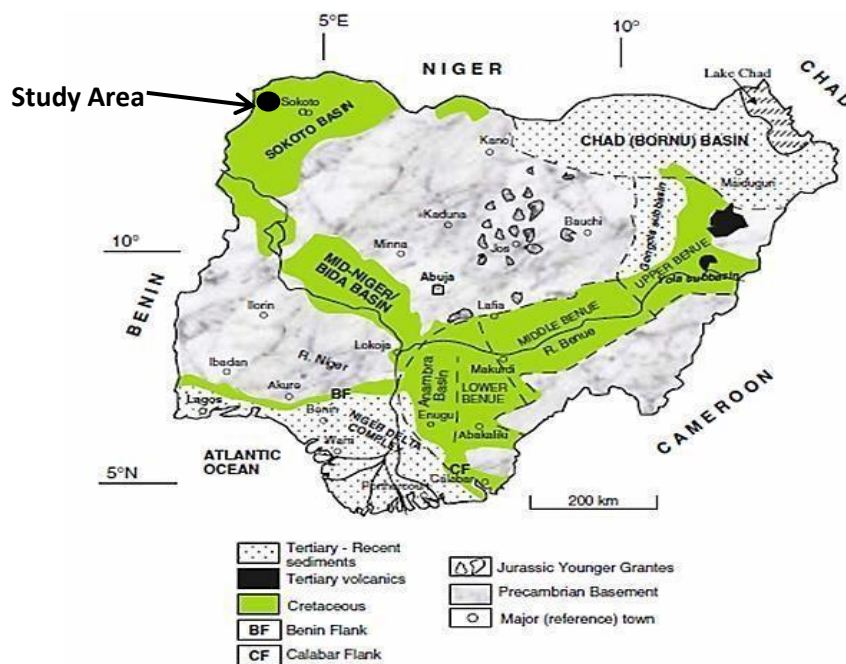


Figure (1) Geology Map of Nigeria showing the Study Area

III. GEOLOGY OF THE STUDY AREA

The Sokoto basin is an embayment of the lullemeden basin which covers a total land area of over 700,000 km² and it is located at Southeastern part of the lullemeden basin and Northwestern part of Nigeria. Stephen, (2018).

Sokoto basin is one of the young Mesozoic tertiary island cretonic sedimentary basin of West Africa. The basin like other intercontinental basin of the region and African continent in general developed by epeinogenetic

warping, stretching and rifting of technically stabilized crust.

The sediments of the lullemeden basin were accumulated during four phases of deposition (Obaje,1987). Overlying the precambrian basement unconformable is Gundumi formation which is made up of drift and clays constituting the premastritian continental intercalaire of West Africa.

They are overlain uncomformably by the mastritian Rima group. Taloka and Wurno formation consisting of mudstone and sandstone

separated by the fossiliferous, Calcareous and ShaleyDukamaje Formation.

The Dange and Gamba formation (mainly shales) separated by the calcareous kalambaina formation constitute the paleocene Sokoto group,

the overlying continental Gwandu formation forms the post Paleocene continental terminal. These sediments deeps gently and thicken gradually toward the Northwest.

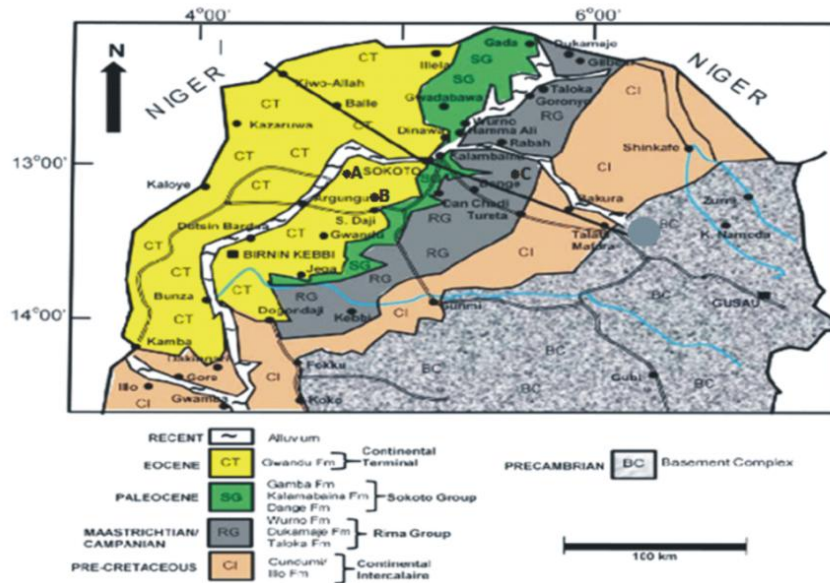


Figure 2. Generalized geological map of the Nigerian sector of the Iullemeden Basin (Sokoto Basin) (Line of Section A-B)

IV. MATERIALS AND METHODS

4.1 Materials

The materials used for the research work includes: the aeromagnetic data obtained from the Nigerian Geological Survey Agency (NGSA), Four (4) high resolution aeromagnetic data sheet covering Binji, sheet (9), Sokoto sheet (10), Argungu sheet (28) and Dangesheet (29).

Software used

Geophysical processing application software such as Oasis Montaj V8.4 from Geosoft, Surfer 13, PC1 Geomatica, Microsoft Excel and Matlab were utilized to performed the analysis

4.2 Data Acquisition

Data acquisition four High resolution Aeromagnetic data of Binji (9), Sokoto (10), Argungu (28), Dange(29) which lies from longitude 4.50°E – 5.50°E to 12.50°N – 13.50°N.

4.2.1 Methodology

The procedure employed in this research includes; This study employed both the qualitative and quantitative interpretation to achieve the aim and objectives of the study. The qualitative interpretation

includes: the interpretation of the total magnetic intensity map of the study area, the residual map, first and second vertical derivative, the quantitative interpretation includes; the interpretation of source parameter imaging map and Euler deconvolution map for depth estimates.

First vertical derivative has almost become a basic necessity in magnetic interpretation projects. In fact, the first vertical derivative is used to delineate high frequency features more clearly where they are shadowed by large amplitude low frequency anomalies. This is done using the Laplace transformation expression shown below:

$$\nabla^2 f = 0 \quad (1)$$

where $\nabla^2 f$ is the Laplace transform which can be expressed in full as:

$$\frac{\partial^2 f}{\partial z^2} = - \left[\frac{\partial^2 f}{\partial x^2} + \frac{\partial^2 f}{\partial y^2} \right] \quad (2)$$

$\partial x, \partial y$ and ∂z are the differentials in x, y and z coordinates

The nth vertical derivative can be computed using:

$$F \left[\frac{\partial^n f}{\partial z^n} \right] = k^n F(f) \quad (3)$$

The second vertical derivative has more resolving power than the first vertical derivative. Apart from enhancing the shallow anomalies, the second vertical

derivatives are also used to delineate geological boundaries between rocks with contrasting physical properties such as magnetic susceptibility. The contoured second vertical derivative outlines the bodies causing the magnetic anomalies (Labbo&Ugodulunwa, 2007). The second vertical derivative is based on equation 3 when $n = 2$ where F is the Fourier representation of the field, k is the wave number or frequency, f is the input to be filtered.

Analytical signal: One advantage of the Analytical Signal technique is that it defines source positions regardless of any remnant magnetization in the sources hence it's independent of the direction of magnetization.

The amplitude of the analytical signal of the total magnetic field F is calculated from the three orthogonal derivative of the field defined as:

$$A(x, y) = \left(\frac{\partial M}{\partial X}\right)X + \left(\frac{\partial M}{\partial Y}\right)Y + \left(\frac{\partial M}{\partial Z}\right)Z \quad (4)$$

With M= magnetic field. The analytical signal Amplitude can now be written as:

$$|A(x, y)| = \sqrt{\left(\frac{\partial M}{\partial X}\right)^2 + \left(\frac{\partial M}{\partial Y}\right)^2 + \left(\frac{\partial M}{\partial Z}\right)^2} \quad (5)$$

4.3 Tilt Derivative:

The tilt derivative filter is defined as

$$TDR = \tan^{-1} \left(\frac{VDR}{THDR} \right) \quad (6)$$

where VDR and THDR are the Vertical derivatives and Tilt horizontal derivatives of the total magnetic intensity respectively.

$$VDR = \frac{\partial T}{\partial z} \text{ and } RHDR = \sqrt{\left(\frac{\partial T}{\partial x}\right)^2 + \left(\frac{\partial T}{\partial y}\right)^2} \quad (7)$$

The total horizontal derivative of the tilt derivative is defined as the square root of the sum of squares of the tilt angle derivatives in the x and y directions and is mathematically defined as:

$$THDR - TDR = \sqrt{\left(\frac{\partial TDR}{\partial x}\right)^2 + \left(\frac{\partial TDR}{\partial y}\right)^2} \quad (8)$$

4.4 Source Parameter Imaging (SPI);

Thurston & Smith (1997) developed source parameter imaging and used it to estimate the depth from the local wave number of the analytical signal. The depth is displayed as an image which makes it better than other depth estimation methods. One more advantage of the source parameter imaging technique is that the estimation of depth is independent of the magnetic inclination, declination, dip, strike and any remnant magnetization (Thurston & Smith, 1997). Hence the technique has been used for depth

estimation of magnetic sources by many authors. Salako (2014), Marwan *et al.*, (2017) and Nwogwugwuet *al.*, (2017) applied it for depth to basement determination. Solution grids using the Source Parameter Imaging technique show the edge location, depth, dips and Susceptibility contrasts.

Thurston and Smith (1997) estimated the depth parameter using the local wave number of the analytic signal. The analytical signal $A_1(X, Z)$ is defined by Nabighian, (1972) as

$$A_1(x, z) = \frac{\partial M(X, Z)}{\partial x} - j \frac{\partial M(X, Z)}{\partial z} \quad (9)$$

where $A_1(x, z)$ = Amplitude of Analytical signal
 $M(x, z)$ = magnitude of the anomalous total magnetic field

j = imaginary number

z and x = are gradients in the vertical and horizontal direction respectively.

Nabighian (1972) also showed that the gradient changes constituting the vertical and horizontal (real and imaginary) parts of the 2D analytical signal are related as follows:

$$\frac{\partial M(X, Z)}{\partial x} \Leftrightarrow -j \frac{\partial M(X, Z)}{\partial z} \quad (10)$$

Where \Leftrightarrow represents a Hilbert transform.

The local wave number k_1 is defined by Thurston & Smith (1972) to be

$$k_1 = \frac{\partial}{\partial x} \tan^{-1} \left[\frac{\frac{\partial M}{\partial z}}{\frac{\partial M}{\partial x}} \right] \quad (11)$$

According to Salako&Nwosu (2014) the signature illustrated by Thurston and Smith (1972) utilized Hilbert transformation pair in (11). The Hilbert transform and vertical derivative operators are linear, so the vertical derivative of (11) will give the Hilbert transform pair as

$$\frac{\partial^2 M(X, Z)}{\partial z \partial x} \Leftrightarrow - \frac{\partial^2 M(X, Z)}{\partial^2 z} \quad (12)$$

Thus the analytic signal could be defined based on second order derivative $A_2(x, z)$

Where

$$A_2(x, z) = \frac{\partial^2 M(X, Z)}{\partial z \partial x} - j \frac{\partial^2 M(X, Z)}{\partial^2 z} \quad (13)$$

This gives rise to a second order local wave number k_2 , where

$$k_2 = \frac{\partial}{\partial x} \tan^{-1} \left[\frac{\frac{\partial^2 M}{\partial^2 z}}{\frac{\partial^2 M}{\partial z \partial x}} \right] \quad (14)$$

The first and second order local wave numbers are used to determine the most appropriate model and

depth estimate independent of any assumption about a model.

4.4.1 Euler De convolution

The Euler De Convolutions a 3-Dimensional semi-automatic interpretation technique widely used in depth estimation and delimitation of a wide variety of geologic structures. It is based on Euler homogeneity equation which relates the potential field (magnetic or gravity) and its gradient components to the location of the sources, by the degree of homogeneity N, interpreted as a structural index.

$$(x-y) \frac{\partial T}{\partial x} + (y-z) \frac{\partial T}{\partial y} + (z-x) \frac{\partial T}{\partial z} = N(B-T) \quad (15)$$

Where T is the total field at (x, y, z) and B is the regional value and N is the structural index. Assuming various measurement point and known N, the above equation can be solved with least squares procedure for unknowns x0, y0, z0 and B. An important parameter in the Euler equation is the structural index N. This is a homogeneity factor relating the magnetic field and its gradient components to the location of the sources. A poor choice of the structural index has been shown to cause a diffuse solution of source locations and serious biases in depth estimation. Both Thompson and Reid suggested that a correct N gives the tightest clustering of the Euler solutions around the geologic structure of interest. Thompson gives more detailed discussion on the degree of homogeneity of potential fields and structural indices of Euler De Convolution.

V. RESULTS AND DISCUSSION

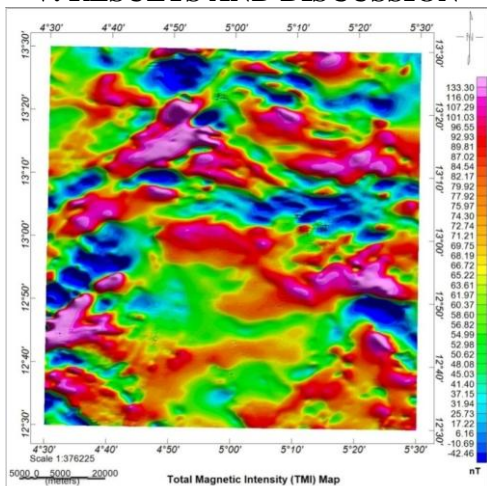


Figure 1: Total Magnetic Intensity Map showing the Study Area

(A sum of 33,000 nT removed for the purpose of handling must be added to get the actual value at any point within the study area).

Figure 1 is the colour image of the IGRF corrected Total magnetic Intensity (TMI) of the study area. The map was produced in aggregate of colours with red to pink signifying high magnetic signatures, yellow representing intermediate between high and low magnetic signature and green to deep blue depicting low magnetic signature. The map is characterised with high and low magnetic signatures and also with long and short wavelength anomalies showing that the study area is composed of crystalline rocks and sediments. The magnetic signatures range from a low of -42.46 nT along western region to some part of northern and south eastern region of the study area, to a high of 133.30 nT in the southwestern, north-eastern and north western parts of the region. To obtain the actual of the magnetic value at any point within the study area, the sum of 33, 000 nT removed for the purpose of handling must be added. Major structures observed on this map trends NE-SW, NW-SE and E-W.

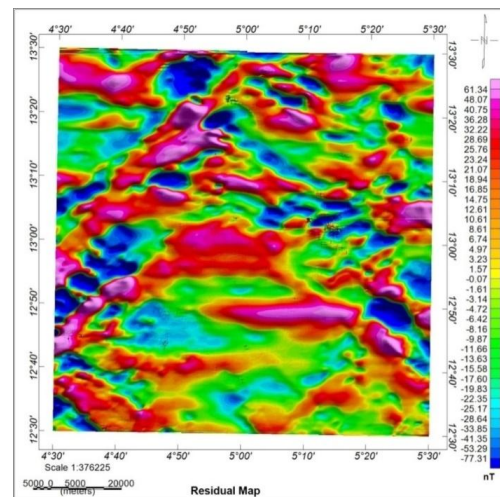


Figure 2: Residual map showing the study area

The residual map (Figure 2) of the study area was produced after removal of the regional field from the total magnetic field of the study area using polynomial fitting so as to remove the effects of the regional field that might overshadow anomalies of interest within the study area. A close look at the map reveals that the map is characterised with high and low magnetic signature with high and low anomalies scattered all over the study area. The magnetic values ranges from -77.31 nT to 61.34 nT. The northern region of the study area is composed of short wavelengths signifying crystalline rocks and the southern part of long wavelength anomalies depicting sedimentary terrain. Magnetic structures (faults, fractures and shear zones) delineated on this map agrees with the ones on Figure 4.1 trending NW-SE, NE-SW and E-W

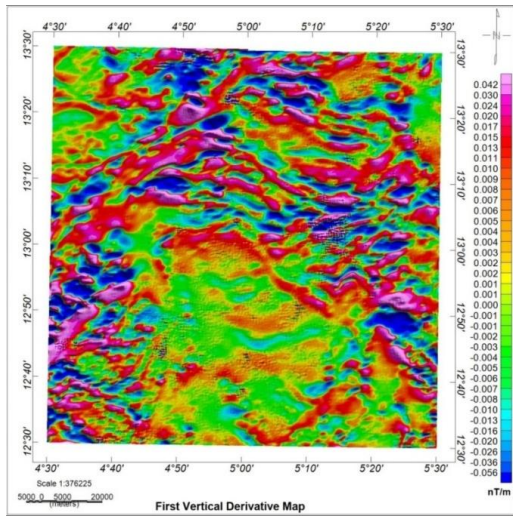


Figure 3a: First vertical derivative map showing the study area

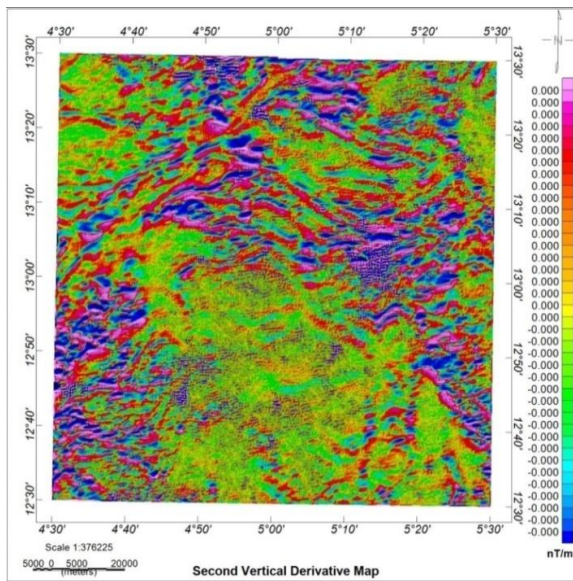


Figure 3b: Second vertical derivative map showing the study area

The vertical derivative maps (Figure 3a and b) gives a good representation of near surface features such as faults (black lines) where the filter enhances short-wavelength anomalies responsible for shallow sources at the expense of long ones. It is outstanding to note that the northern, southwestern and south-eastern part of the study area was occupied by such short-wavelength anomalies indicating a relatively shallow depth of the causative sources viz-a-viz the southern part where it can be concluded a deeper sources conformable with the presence of a sedimentary cover. Visual inspection on the two maps show that major structures which might host

potential minerals within the study area observed on the maps trend NW-SE, NE-SW, E-S and N-S with NW-SE and NE-SW more pronounced. These trending agrees with ones on Figure 1 and Figure 2.

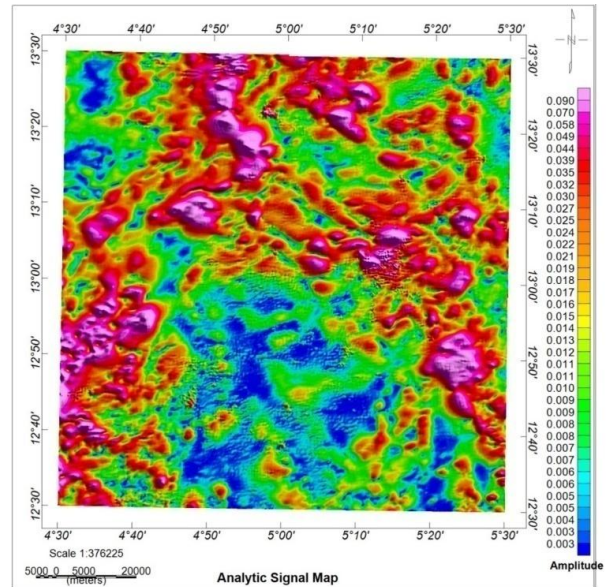


Figure 4: Analytic signal map showing the study area

The analytical signal map (Figure 4) enhances the variation in the magnetization of the magnetic sources in the study area and highlights discontinuities and anomaly texture. On comparison with FVD and SVD (Figure 3a and 3b) the differentiated and undifferentiated complexes have been redefined and properly mapped not only based on their depths but mineralogical compositions as well. Consequently, the high magnetic anomalies zones are associated with highly rich ferromagnesian-bearing rocks with minor felsic minerals (Telford et al., 1990). Therefore, analytic signal map unveiled three different magnetic zones. Low to fairly low magnetic zone with a gradient 0.003–0.013 amplitude (nT/km) associated with clastic sediments, metavolcanic, metasediments, and granite because these rocks contain more than 60% quartz. The moderate zone with gradient 0.017-0.030 amplitude (nT/km) associated with granite – gneiss as these rocks contain high ferromagnesian with low amount of felsic minerals. The high magnetic anomalies zones 0.032–0.090 amplitude (nT/km) are related to ophiolitic serpentine, ophioliticmetagabbro, gabbroic rocks, as these rocks have high ferromagnesian with large amount of felsic minerals (Elkhateeb and Abdellatif, 2018).

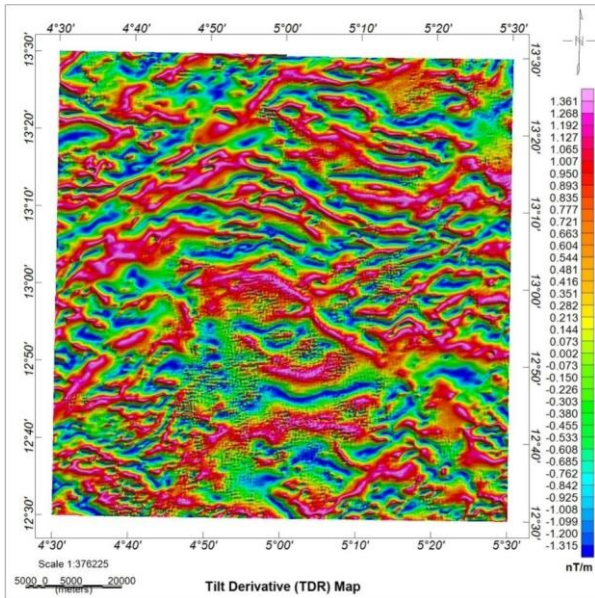


Figure 5: Tilt derivative (TDR) map showing the study area

The tilt derivative map (Figure 5) accentuate short wavelength anomalies and very useful in mapping shallow basement structures/near-surface features and mineral exploration targets (Adewumi and Salako, 2018). The map (Figure 5) corroborates with the previous discussed maps (Figure 4.1, 4.2, 4.3 and 4.4). It reveals structures (faults, fractures and shear zones) that might host solid minerals in the northern, south-western and south-eastern part of the study area since minerals are structurally control. These structures trends NE-SW, NW-SE and E-W.

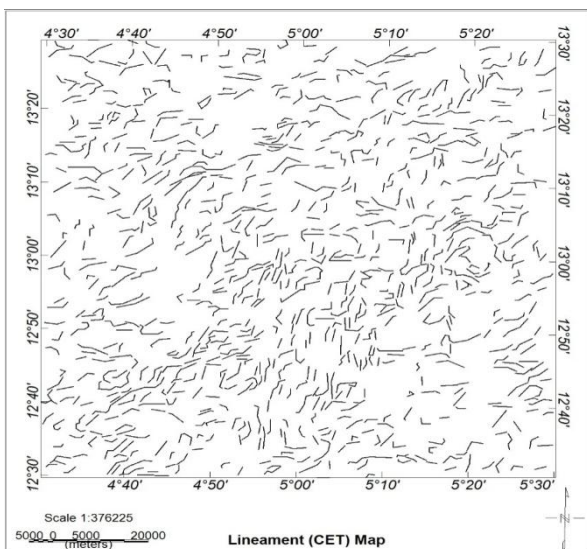


Figure 6: Lineament map (CET) showing the study area

This was carried out to identify linear structures contained within the aeromagnetic data via consecutive map by-product forms that include standard deviation which estimates magnetic variations, then phase symmetry to separate laterally continuous lines. Thereafter, the resulted lineaments enhanced by suppressing noise and background signals using an amplitude thresholding (Figure 7).

It is worth mentioning that the lineaments revealed by the Vectorisation map (Figure 7) reveal the basement rocks that occupy the northern, south-western and south-eastern part of the area are highly deformed as compared with the southern part covered by cretaceous sandstone. The map reveals NW-SE and NE-SW prominent trending with minor E-W and N-S trending.

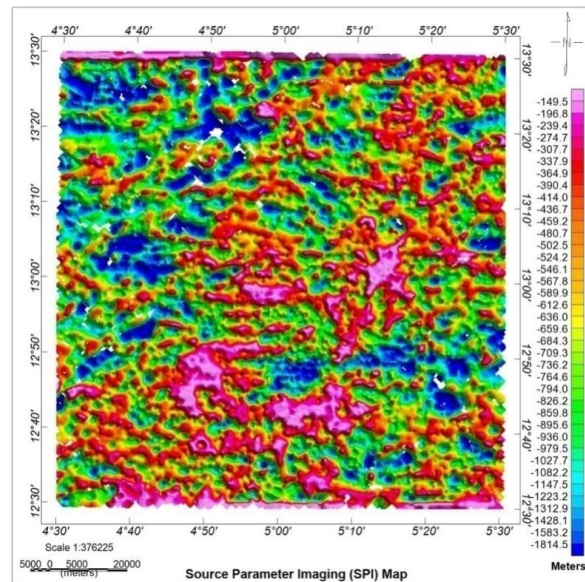


Figure 7: Source Parameter Imaging (SPI) map showing the study area

The depth to magnetic basement was obtained using source parameter imaging. This was used because it gives a clearer picture of the anomalies with their respective depths. The map (Figure 8) reveals sediment depicted with green to deep blue colour with an average thickness of 1.8 km and even more at the southern portion of the study area. While the basement region depicted with red to pink colour reveals average depth of 0.14 km at the northern, southwestern and southeastern part of the study area. This map also agree with the analytic signal map (Figure 5) with regions of shallow depth corresponding to regions of high magnetic amplitude anomalies and regions of thick sedimentation corresponding to regions of low magnetic amplitude anomalies. Since structures within the crystalline rocks are the host of some magnetic minerals, the

average depth at which this could be located is about 0.14 km. The vertical derivative maps attest to this fact; that the shallow wavelength anomalies are closer to the surface.

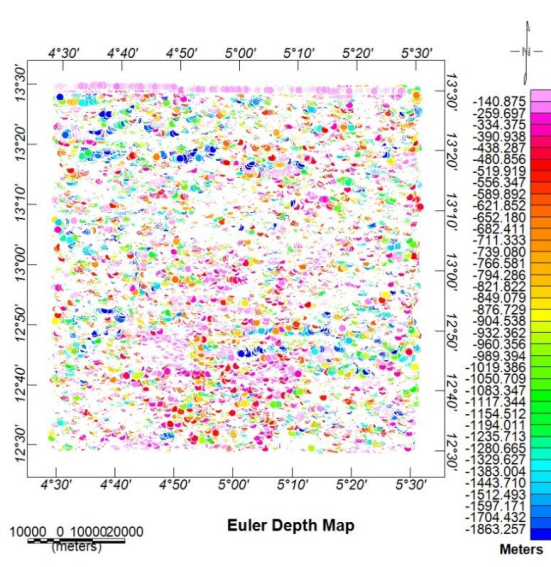


Figure 8: Euler Depth map showing the study area

The Euler deconvolution method of depth determination is an automatic technique used for locating source of potential field based on amplitudes and gradients; it windows the area and locates structures and evaluate the depth to which those structures exist by writing equations for the structures. Its degree of accuracy depends on the structures having a perfect shape and that the structure or anomaly falls on the center of the window. Figures 8 represent the map for the Euler depth. The Euler Depth map shows that the depth to magnetic sources (anomalies) ranges from 140.87 m to 1863.25 m. the thickness of sediments and shallow depth obtained from this map corroborate with ones obtained from source parameter imaging (Figure 4.8). Since structures within the crystalline rocks are the host of some magnetic minerals, the average depth at which this could be located is about 0.14 km. The vertical derivative maps attest to this fact; that the shallow wavelength anomalies are closer to the surface.

V. DISCUSSION

Subsurface investigation of solid mineral in the northeastern part of Sokoto basin using qualitative and quantitative analysis of aeromagnetic data has been successfully carried out with the purpose of delineating possible mineralization zones within the study area on a reconnaissance basis.

The total magnetic intensity map of the study area reveals variation in magnetic intensity rising from variation in the magnetic susceptibility of the rocks in the study area. The magnetic intensity value ranges from -42.46 nT to 133.30 nT. Regions of high magnetic signatures attributable to crystalline basement might host the solid minerals (like Phosphate) within the study area.

The residual map reveals variation in magnetic signatures with the magnetic value ranging from -77.31 nT to 61.34 nT. Just like the TMI, Regions of high magnetic signatures attributable to crystalline basement rocks might host the solid minerals (like Phosphate) within the study area.

The first and second vertical derivative map reveals shallow geological structures which might host solid mineral within the study area since magnetic minerals are structurally control. Dominant structures (faults, fractures) trends NW-SE and NE-SW and minor structures trending E-W and N-S.

The analytic signal map reveals Low to fairly low magnetic zone with a gradient 0.003–0.013 amplitude (nT/km) associated with clastic sediments, metavolcanic, metasediments, and granite because these rocks contain more than 60% quartz. The moderate zone with gradient 0.017-0.030 amplitude (nT/km) associated with granite – gneiss as these rocks contain high ferromagnesian with low amount of felsic minerals. The high magnetic anomalies zones 0.032–0.090 amplitude (nT/km) are related to ophiolitic serpentine, ophioliticmetagabbro, gabbroic rocks, as these rocks have high ferromagnesian with large amount of felsic minerals.

The tilt derivative map reveals structures (faults, fractures and shear zones) that might host solid minerals in the northern, south-western and south-eastern part of the study area since minerals are structurally control. These structures trends NE-SW, NW-SE and E-W.

The Lineament map from centre for exploration targeting shows that lineaments (faults, fractures that host solid minerals) revealed by the Vectorisation map (Figure 4.7) reveal the basement rocks that occupy the northern, south-western and south-eastern part of the area are highly deformed as compared with the southern part covered by sediments. The map reveals NW-SE and NE-SW prominent trending with minor E-W and N-S trending.

The two depth estimating techniques (Source Parameter Imaging and Euler Deconvolution) employed in this study reveal thickness of sediments depicted with an average thickness of 1.8 km and shallow depth of 0.14 km at the northern, southwestern and southeastern part of the study area. Since structures within the crystalline

rocks are the host of some magnetic minerals, the average depth at which this could be located is about 0.14 km. The vertical derivative maps confirm this fact; that the shallow wavelength anomalies are closer to the surface.

VI. CONCLUSION

In conclusion, from the results of the analysis and interpretation of aeromagnetic data of part of Sokoto basin with the aim of investigating the subsurface structures for solid mineral in the study area, it therefore be stated that regions of possible mineralisation and the depth at which they can be explored has been successfully delineated in this study.

REFERENCE

- [1]. Aigbedion, I, &Iyayi, S.E (2007).Environmental effect of mineral exploitation in Nigeria International Journal of Physical Sciences, 2(2), 33-38.
- [2]. Eze Mo, Mamah L.I, Madu AJC, Leonard O. (2011). Geological and structural interpretation of possible mineralization zones of part of Anambra Basin and Southern Benue through using airborne geophysical data. International Journal of Research in Engineering and Applies Science 7(5): 70-80.
- [3]. Labbo, A.Z. &Ugodulunwa, F.O (2007). An interpretation of total intensity Aeromagnetic maps of part of Southeastern Sokoto basin. Journal of Engineering and applied sciences 3,1, 15-20.
- [4]. Marwan, A.A and Yahia M.A, (2017). Using the Aeromagnetic Data for Mapping the Basement Depth and connect locations at Southern part of Tihemah Region, Yemen. Egyptian Journal and contact of petroleum <https://dx.doi.org/10.1016/j.ejpe.07.015>. Retrieved December 20, 2017 from www.sciencedirection.com
- [5]. Nabighian MN (1972). The analytic signal of two dimensional magnetic bodies with polygonal cross section: its properties and use for automated anomaly interpretation Geophysics 37:507.
- [6]. Obaje, N. G. (1987). Foraminiferal biostratigraphy and paleoenvironment of the Sokoto Basin of NW Nigeria.M. Sc Thesis, Ahmadu Bello University, Zaria, 76pp.
- [7]. Reeves, C. (2005).Aeromagnetic Surveys Principles Practice and Interpretation Geosoft.I.2-17.
- [8]. Sada, MM, (2013). Mid-term report for the minerals and metals sector Nigeria Ministry of Mines and Steel Development, <http://slideshow.net> landbank/Ministry of Mines and Steel Development Sajini F.I, (2013).Socio-economic problems of oil exploration and exploitation in Nigeria's Niger Journal of Energy Technologies and Policy. 3(3) SSN222 4-3232.
- [9]. Salako, K. A., and Udensi, E. E. (2013).Spectral Depth Analysis of Parts of Upper Benue Trough and Borno Basin, North-East Nigeria, Using Aeromagnetic Data.*International Journal of Science and Research*, 2(8), 2319-7064.
- [10]. Stephen O. and UcheIduma (2018).Structural Interpretation of Northern Sokoto Basin, Using Airborne Magnetic Data.*International Journal of Innovative Research in Science, Engineering and Technology*, Vol. 7(7) pp 8041-8048.
- [11]. Thompson, D.T. (1982). A new technique for making computer assisted depth estimates from magnetic data Geophysics. 47, 31-37.
- [12]. Thurston, JB, Smith, RS. Automatic conversion of magnetic data to depth, dip, and susceptibility contrast using the SPITM method. Geophysics. 1997, 62, 807-813.